Kochi Chapter

Indian Geotechnical Conference
IGC 2022
15th – 17th December, 2022, Kochi

Three Dimensional Responses of Tunnel to Adjacent Construction

M. Vinoth[1[0000-0002-1992-2801]] and Aswathy M.S[1[0000-0002-1241-7001]]

[1] CSIR-Central Building Research Institute, Roorkee, India
Vinothm.27@gmail.com

Abstract. Adjacent construction activities, such as deep excavations for basement construction, will result in stress changes that will eventually result in subsurface movement, potentially disrupting existing tunnels. The effects of clear depth below the bottom of the excavation on the adjacent tunnel due to deep excavation in a homogeneous sandy stratum have been addressed in this paper. A number of Three Dimensional FE analyses were carried out to examine the impacts of deep excavation on the existing adjacent tunnel. Numerical analysis was performed using an advanced soil constitutive Hardening Soil model with small-strain stiffness (HSS) to capture the complex interaction behaviour between deep excavation and tunnel. Investigations have been made into the induced tunnel deformation and strain in both transverse and longitudinal directions. The same study was extended to investigate the tunnel's response to the adjacent deep excavation in stratified soil. Deformations and strains obtained from homogeneous strata are under estimated in relation to those obtained from stratified soils.

Keywords: Tunnelling; deep excavation; FEM

1 Introduction

Due to the rapidly growing urban population, the need to build a transportation system for this growing population has led to the use of underground space. Construction of a new subsurface structure, particularly a basement with large excavations, may affect existing adjacent subsurface structures, such as tunnels, as a result of changes in stress. Such stress changes may have an impact on the structural integrity of the existing tunnel.

Excavations cause stress release which eventually lead movement of existing tunnel in both longitudinal and transverse direction. Most of the existing work [1, 2, 3, 4, 5] has been performed taking into account the interaction between the excavation and tunnel as a plane strain condition. [6] developed a formula for determining the heave of existing tunnels due to adjacent construction in soft clay soil. Research work of [7] brought out, as long as the size of the underground excavation along the longitudinal direction of the tunnel exceeds 9 times the excavation depth, the behaviour of the basement excavation-tunnel cannot be simplified as a plane strain condition. So, when the excavation depth is smaller than nine times the depth of the excavation, it is mandatory to take into account the 3 Dimensional responses of the existing tunnel. Past research suggests that there is certainly an interaction between the excavation and

existing tunnel structure that would greatly affect the existing underlying tunnel and soil settlement at the ground surface.
In this paper, in order to determine the three-dimensional effect of clear depth, space between the excavation bottom and tunnel crown, given the size of the excavation is nine times less than excavation depth was investigated. Three-dimensional numerical model was developed in the MIDAS GTS-NX finite element software. Detailed study was performed using homogeneous soil condition and later it was extended to stratified soil condition. Construction sequence adopted in the field was simulated accurately in the developed numerical model. The structural response of the existing tunnel due to adjacent excavation is assessed.

2 Numerical studies of the excavation-tunnel interaction

2.1 Finite element analysis model and limit conditions

Three-dimensional numerical model has been developed and analysed in a finite element software, MIDAS GTS-NX. The model size is 175 m (length) × 175 m (breadth) × 50 m (depth) has been selected to minimise boundary effects (refer Fig. 1). The overall depth of the model (50 m) was chosen to be five times higher than the maximum depth of excavation recommended by[8]. The effect of the tunnel construction was not accounted for in the model, tunnel was simulated by wish in-place approach. Boundary conditions, bottom it is restrained to move in all the three directions, on four sides, it is restrained to move in both horizontal directions and free to move in vertical direction.
The existing tunnel was modeled as 2D shell elements, in order to take effects of joints in to account, the stiffness of the tunnel lining was reduced to 80% of the actual capacity [9]. Diaphragm wall (D-Wall) was used for retaining the soil during excavation was modeled as a 2D shell element. Soil was modeled as a 3D solid element. For all elements a 'Hybrid Mesher (Hexahedron centered)' has been used. The size of the mesh for tunnel lining and diaphragm wall was kept at 1 and 4 for soil. The clear depth 'Z_c' below bottom of the excavation was varied between 5 m and 9 m (refer Fig. 2).

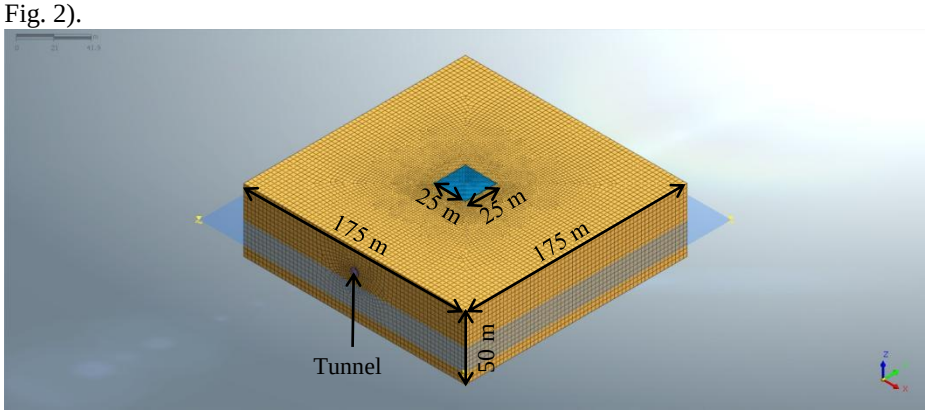

Fig. 1. Typical numerical model developed in MIDAS GTS-NX.

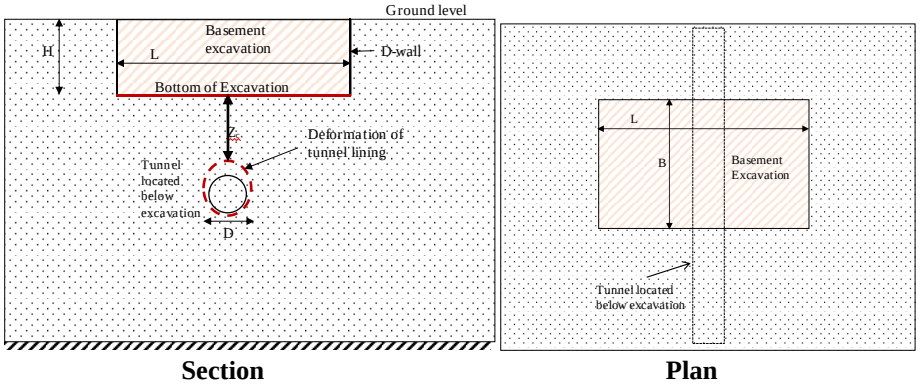

Fig. 2. Schematic representation of the case considered for study.

2.2 Model and input parameters

Tunnel lining and diaphragm wall were considered to be isotropic-elastic structural materials. An 800 mm thick cantilever diaphragm wall was taken into account in the present study. The depth of diaphragm wall was 13.5 m with a embedment depth of 4.5m. Embedment depth was considered to be 50% of total excavation depth (H) as suggested by [10]. Soil was modeled using hardening soil with small strain stiffness model. Soil and tunnel data was obtained from the geotechnical investigation carried for one of the Delhi Metro Rail Corporation (DMRC). Structural and soil component properties are presented in Table 1 and Table 2 respectively. M30 grade was assumed for D-Wall concrete and, based on DMRC data, M50 grade was used for lining. Using Eq.1 young's modulus was determined. Taking into account the joints in the lining segments, the stiffness of the lining has been reduced to 75%. The friction angle was obtained from the DMRC geotechnical investigation report. The size of the tunnel was selected from the data obtained from DMRC, the outer and inner diameter of tunnel were 6.3 m and 5.8 m respectively. In all cases, the groundwater was considered to be below invert level of the tunnel. To investigate the behaviour of the existing tunnel due to adjacent excavation, homogeneous silty soil (ML) was assumed in the study. The size of excavation considered in the study is 25 m (length) × 25 m (breadth) × 9 m (depth).

$$E = 5000\sqrt{f_{ck}} \quad (1)$$

f_{ck} - characteristic compressive strength of concrete

Table 1. Material properties of diaphragm wall and lining.

Parameter	D-Wall	Lining
Material weight, kN/m^3	25	25
Young's modulus, E kPa	27386127.9	26516504.3
Poisson's ratio	0.2	0.15

Table 2. Soil properties for HSS model.

Parameter	ML	Unit

Parameter	ML	Unit
Unsaturated unit weight, γ_{unsat}	16.5	kN/m^3
Saturated unit weight, γ_{sat}	18.6	kN/m^3
Friction angle, φ	31.8	°
Dilatancy angle, ψ	1.8	°
Cohesion, c_{ref}	4.6	kPa
Initial void ratio, e_0	0.6	-
Reference secant stiffness in triaxial test, E_{50}^{ref} [$\times 10^4$]	11.58	kPa
Reference tangent stiffness for oedometer loading, E_{oed}^{ref} [$\times 10^4$]	11.58	kPa
Reference unloading/reloading Stiffness, E_{ur}^{ref} [$\times 10^4$]	34.75	kPa
Power for stress dependency of stiffness, m	0.5	-
Coefficient of Permeability, $k_x=k_y$ [$\times 10^{-2}$]	5×10^{-5}	m/sec
Coefficient of Permeability, k_z [$\times 10^{-2}$]	1.67×10^{-5}	m/sec
Reference shear modulus at very small strains, G_0^{ref}	459422	kPa
Shear strain, $\gamma_{0.7}$ [$\times 10^{-5}$]	4.73	-
Poisson's Ratio, υ	0.3	-
Reference stress, p^{ref}	100	kPa

2.3 Staged construction

In the first stage, in-situ stress was generated and followed by tunnel activation. The deformation caused due to in-situ stress and installation of tunnel were ignored and deformation was reset to zero prior to installation of diaphragm wall. In the next step installation of diaphragm wall was simulated. After D-Wall installation, staged excavation was initiated by deactivating the soil in depths of 2 m except last stage, where only 1 m soil was deactivated. The steps involved in the numerical simulation is provided in the Table 3.

Table 3. Steps followed in numerical simulation.

Step	Description
1	Initial stress generation
2	Activation of existing tunnel
3	Installation of diaphragm wall
4	Removal of soil up to -2 m
5	Removal of soil up to -4 m
6	Removal of soil up to -6 m
7	Removal of soil up to -8 m
8	Removal of soil up to -9 m

3 Results and discussions

3.1 Homogeneous stratum

Deformation in transverse direction

Fig. 3 shows the variation of the tunnel size in the cross-sectional direction for the variation of clear depth (Z_c) with unloading factor (E_d/D), where E_d denotes the excavation depth and D the tunnel outer diameter. Positive and negative values concern the extension and compression of the tunnels respectively. 14-V and 14-H indicate that the depth of cover of the tunnel is 14m and V/H denotes deformation in tunnel along crown-invert axis and left-right springline respectively. Similarly the plot is prepared for other cover depths. In all the cases, elongation has been observed in the crown-invert axis and compression along the tunnel springlines. This is due to the reduction of vertical stresses from excavation and relatively less reduction of horizontal stress. As the depth of excavation increases, the magnitude of elongation and compression also increases. On final excavation stage, elongation and compression were maximum in the case where Z_c was 5 m and decreased by an amount of 24% and 23% respectively, while Z_c increased to 9 m. The reason for the decrease in elongation and compression as the Z_c increases is the availability of an additional overburden pressure to counteract the reduction in vertical stress.

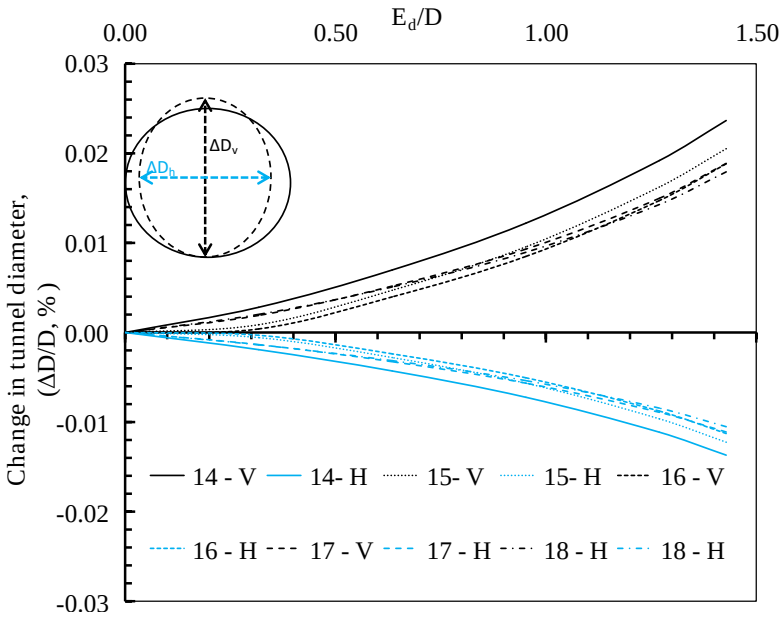

Fig. 3. Deformation of tunnel in transverse direction for different Z_c

Deformation in longitudinal direction

Fig. 4 shows the distortion of the tunnel along longitudinal direction for varying clear depth (C) with unloading factor. It can be deduced from the Fig. 4 that the heave was

induced in the tunnel along the longitudinal direction because of the relieving of stresses from the excavation above the existing tunnel. After reaching maximum excavation depth ($E_{d,max}$ = 9 m), the maximum heave obtained is 0.028 E_d% (E_d = maximum excavation depth), where the crown is 14 m below ground level. As the location of crown moved further deeper to 18 m below ground level, maximum heave in the tunnel has reduced to 0.02 Ed%. The maximum heave was observed just below the centre of excavation and gradually decreases as moved away from the centre of excavation. At a distance of 2.5 times B/2, the impact of the excavation on tunnel was not observed.

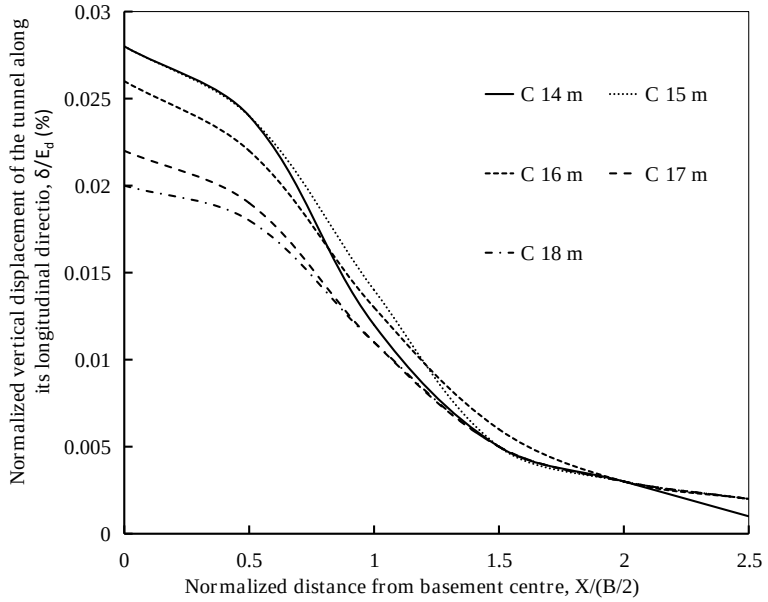

Fig. 4. Deformation of tunnel in longitudinal direction for different Z_c

Strain in transverse direction

Induced strain in tunnel in the transverse direction for varying clear depth (C) with unloading factor is shown in Fig. 5. The strains shown in Fig. 5 are additional, i.e., because of the adjacent deep excavation alone. Positive and negative values concern respectively the tension and compression strains. Since the basement excavation caused symmetrical stress relief, the shape of the strains obtained from the numerical analysis is symmetrical. Except in springline in all other locations tensile strains were induced. Such response suggests that compression occurs at springline and tension at other locations. The maximum tensile (31 με) and compressive strains (40 με) were obtained when the clear depth(Z_c) was 5 m. As the depth of Z_c was increased to 9 m, both compressive and tensile strains were reduced to 32 με and 22 με respectively.

Strain in longitudinal direction

Longitudinal strains induced in tunnel for varying clear depth (C) with unloading factor is shown in Fig. 6. Tension and compression strains observed at tunnel crown are denoted by positive and negative values respectively. In addition, hogging and sagging denote tension and compression strains occurring at tunnel crown, respectively. As expected, the profile of strains is symmetric because of the symmetrical relieving of the stress of the basement excavation. Since the heave was not uniform along the longitudinal direction (refer Fig. 4), hogging and sagging are induced in the tunnel. It can be noted that in all cases examined in this study, the inflection point (i.e., zero strain) is on the excavation boundary. It can be deduced from the Fig. 6, tensile strain is observed below bottom of excavation and compressive strains elsewhere. A maximum tensile strain of 17 με was observed when Z_c is 5 m and reduced to 1.4 με when Z_c was increased to 9 m.

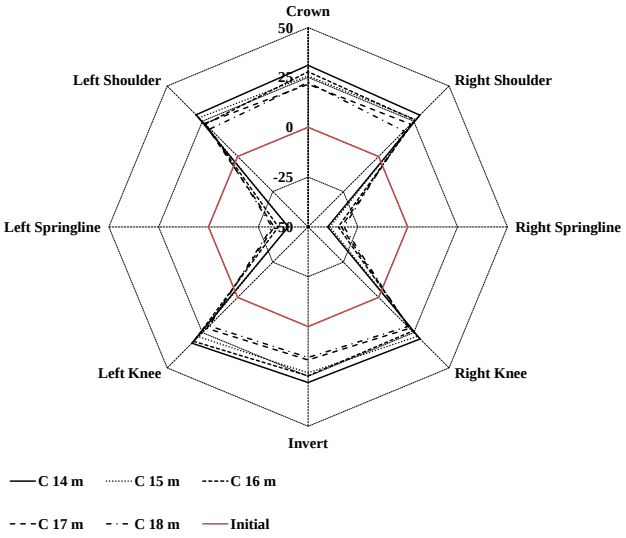

Fig. 5. Strain in tunnel along transverse direction for different Z_c

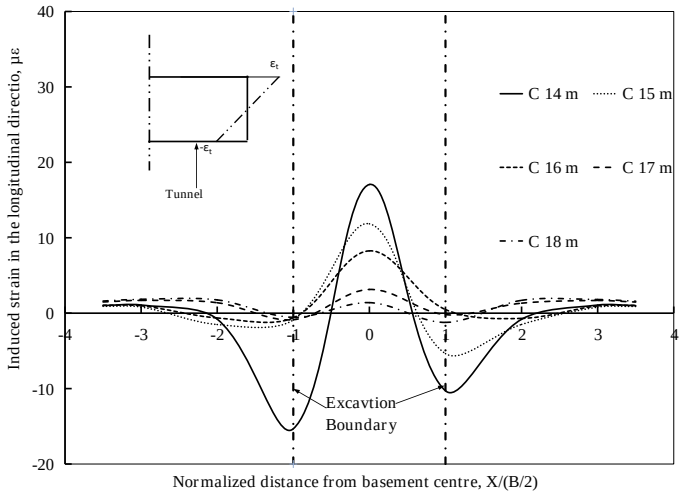

Fig. 6. Longitudinal strain induced in tunnel for different Z_c

3.2 Stratified soil

Further studies were conducted to assess the behaviour of tunnel to deep excavation in the stratified soil stratum. To perform the comparison study, crown at 14 m case was utilized. Deformation and strain variation along transverse and longitudinal direction were taken into account (refer Fig. 7 to Fig. 10). It can be inferred from these Fig. 7 to Fig. 10, higher deformation and strains are obtained when the numerical analysis was carried using stratified stratum when compared to homogeneous soil stratum.

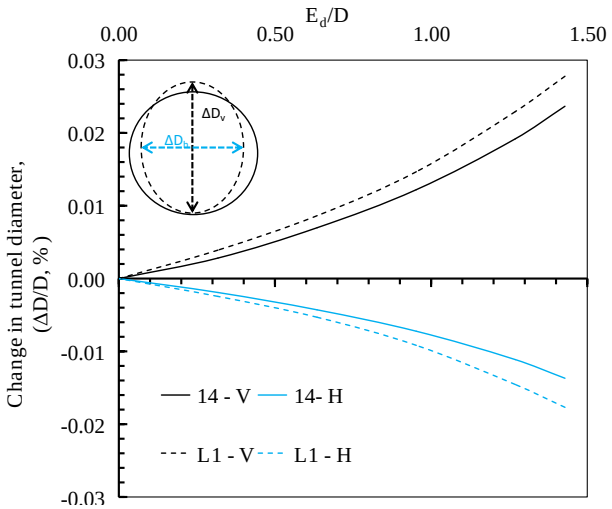

Fig. 7. Comparison of deformation of tunnel in transverse direction between homogeneous and layered stratum for different Z_c

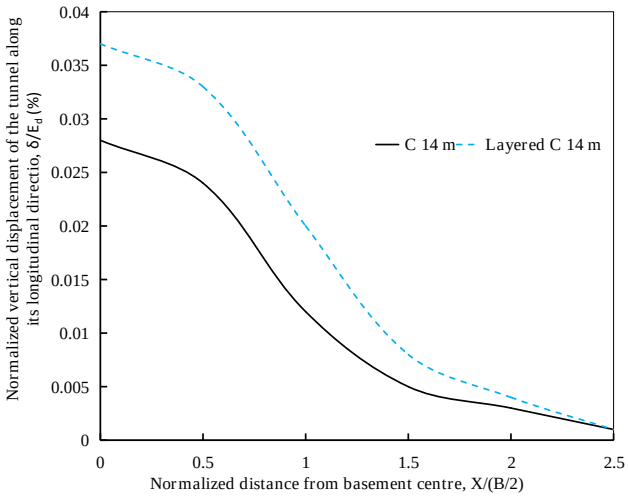

Fig. 8. Comparison of deformation of tunnel in longitudinal direction between homogeneous and layered stratum for different Z_c

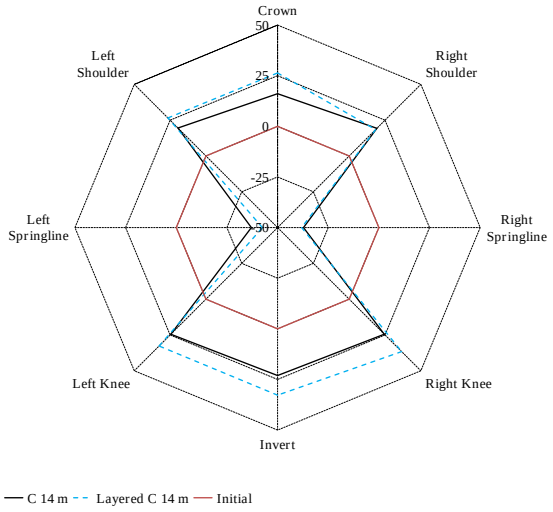

Fig. 9. Comparison of strain in transverse direction between homogeneous and layered stratum for different Z_c

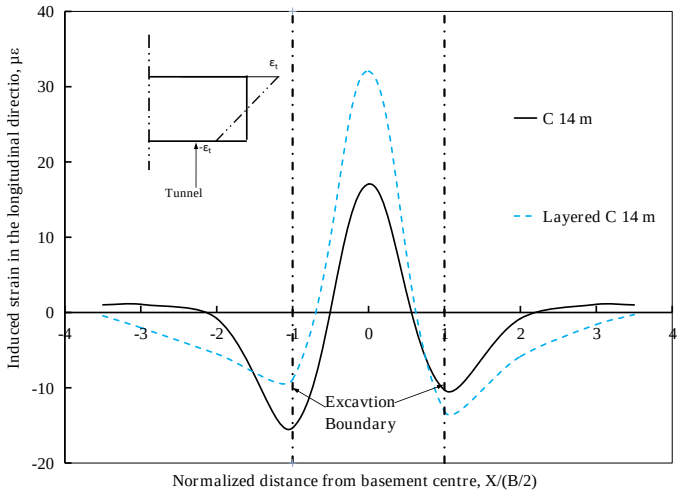

Fig. 10. Comparison of longitudinal strain in tunnel between homogeneous and layered stratum for different Z_c

A maximum elongation of 1.75 D% was obtained in the transverse direction when stratified soil stratum was used as opposed to 1.49 D% in homogeneous soil. Elongation along longitudinal direction increased by 32% in stratified soil condition. Maximum tensile strain increased from 31 με to 36 με in transverse direction when layered soil is used in place of homogeneous soil condition. A 47% increase in the tensile strain at the crown in longitudinal direction was observed in stratified soil when compared to homogeneous soil condition.
Therefore, it can be interpreted from the results that the homogeneous soil condition underestimated the deformations and strains developed in the tunnel due to adjacent excavation.

4 Conclusion

In the present study effect of adjacent excavation on underlying existing tunnel was considered. Following are the findings from the present study,

- Excavation depth and the magnitude of elongation and compression are directly proportional.
- The maximum heave was observed just below the centre of excavation and gradually decreases as moved away from the centre of excavation and becomes negligible at a distance of 2.5 times B/2.
- Except in springline in all other locations tensile strains were induced.
- The inflection point (i.e., zero strain) was found to be on the excavation boundary.
- Higher deformation and strains are obtained for stratified stratum when compared to homogeneous soil stratum.

References

1. Dolezalova M. Tunnel complex unloaded by a deep excavation. Computers and Geotechnics, 2001, 28(3): 469−493.
2. Hu Z F, Yue Z Q, Zhou J, Tham L G. Design and construction of a deep excavation in soft soils adjacent to the Shanghai Metro tunnels. Canadian Geotechnical Journal, 2003, 40(5): 933−948.
3. Zheng, G., Wei, S.W. Numerical analyses of influence of overlying pit excavation on existing tunnels. J. Central South Univ. Technol, 2008, 15 (S2), 69–75.
4. Zheng G, Du YM, Cheng XS, Diao Y, Deng X, Wang FJ. Characteristics and prediction methods for tunnel deformations induced by excavations. Geomech Eng 2017;12(3):361–97.
5. Gang Zheng, Xinyu Yang, Haizuo Zhou, Yiming Du, Jiayu Sun, Xiaoxuan Yu, A simplified prediction method for evaluating tunnel displacement induced by laterally adjacent excavations, Computers and Geotechnics, 2018, 95, 119-128.
6. Huang, A.J., Wang, D.Y., Wang, Z.X. Rebound effects of running tunnels underneath an excavation. Tunnelling and Underground Space Technology, 2006, 21 (3–4), 399–405.
7. Shi, J., Ng, C.W.W., Chen, Y.H. Three-dimensional numerical parametric study of the influence of basement excavation on existing tunnel. Comput. Geotech., 2015, 63, 146–158.
8. Ming-Guang Li, Xiao Xiao, Jian-Hua Wang, Jin-Jian Chen, Numerical study on responses of an existing metro line to staged deep excavations, Tunnelling and Underground Space Technology, 2019, 85, 268-281.
9. Lim, A., Ou, C-Y., Hsieh, P-G. Evaluation Clay of Constitutive Models for Analysis of Deep Excavation under Undrained Conditions. Journal of GeoEngineering, 2010, 5(1), 9–20.
10. Burt Look, Handbook of Geotechnical Investigation and Design Tables, Taylor & Francis, London, 2007.